ROUTING AND ACTION

MEMORANDUM

ROUTING

TO:(1) Electromagnetic Spectrum Sciences Branch (EMSS) (Harvey, James)

Report is available for review

(2) Proposal Files Report No.: -PCS Proposal Number: 65928-EM-PCS.9

DESCRIPTION OF MATERIAL

CONTRACT OR GRANT NUMBER: W911NF-17-1-0204

INSTITUTION: California Institute of Technology

PRINCIPAL INVESTIGATOR: David Hsieh

TYPE REPORT: Final Report

DATE RECEIVED: 7/16/23 9:19AM

PERIOD COVERED: 4/15/17 12:00AM through 4/14/23 12:00AM

TITLE: Final Report: Novel Quantum Phases in Heavy d- and f-electron Systems Studied Using Nonlinear Optics

ACTION TAKEN BY DIVISION

(x) Report has been reviewed for technical sufficiency and IS [x] IS NOT [ ] satisfactory.

(x) Based on my technical review, I have identified no OPSEC or Technology Protection concerns that need to be addressed regarding this report.

(x) Perfomance of the research effort was accomplished in a satisfactory manner and all other technical requirements have been fulfilled.

(x) Based upon my knowledge of the research project, I agree with the patent information disclosed.

Approved by SSL\JAMES.F.HARVEY on 7/31/23 5:26PM

ARO FORM 36-E

REPORT DOCUMENTATION PAGE

Form Approved OMB NO. 0704-0188

1. REPORT DATE (DD-MM-YYYY)	2. REPORT TYPE	3. DATES COVERED (From - To)
16-07-2023	Final Report	15-Apr-2017 - 14-Apr-2023

4. TITLE AND SUBTITLE
Final Report: Novel Quantum Phases in Heavy d- and f-electron Systems Studied Using Nonlinear Optics

5a. CONTRACT NUMBER
W911NF-17-1-0204

5b. GRANT NUMBER

5c. PROGRAM ELEMENT NUMBER
611103

6. AUTHORS

5d. PROJECT NUMBER

5e. TASK NUMBER

5f. WORK UNIT NUMBER

7. PERFORMING ORGANIZATION NAMES AND ADDRESSES
California Institute of Technology
1200 E. California Blvd.
Office of Sponsored Research
Pasadena, CA 91125 -0001

8. PERFORMING ORGANIZATION REPORT NUMBER

9. SPONSORING/MONITORING AGENCY NAME(S) AND ADDRESS (ES)
U.S. Army Research Office
P.O. Box 12211
Research Triangle Park, NC 27709-2211

10. SPONSOR/MONITOR'S ACRONYM(S)
ARO

11. SPONSOR/MONITOR'S REPORT NUMBER(S)
65928-EM-PCS.9

12. DISTRIBUTION AVAILIBILITY STATEMENT
Approved for public release; distribution is unlimited.

13. SUPPLEMENTARY NOTES
The views, opinions and/or findings contained in this report are those of the author(s) and should not contrued as an official Department of the Army position, policy or decision, unless so designated by other documentation.

14. ABSTRACT

15. SUBJECT TERMS

16. SECURITY CLASSIFICATION OF:			17. LIMITATION OF ABSTRACT	15. NUMBER OF PAGES	19a. NAME OF RESPONSIBLE PERSON
a. REPORT	b. ABSTRACT	c. THIS PAGE			David Hsieh
UU	UU	UU	UU		19b. TELEPHONE NUMBER 626-395-4758

RPPR Final Report
as of 31-Jul-2023

Agency Code: 21XD

Proposal Number: 65928EMPCS **Agreement Number: W911NF-17-1-0204**
INVESTIGATOR(S):

Name: David Hsieh
Email: dhsieh@caltech.edu
Phone Number: 6263954758
Principal: Y

Organization: **California Institute of Technology**
Address: 1200 E. California Blvd., Pasadena, CA 911250001
Country: USA
DUNS Number: 009584210 EIN: 951643307

Report Date: 14-Jul-2023 Date Received: 16-Jul-2023
Final Report for Period Beginning 15-Apr-2017 and Ending 14-Apr-2023
Title: Novel Quantum Phases in Heavy d- and f-electron Systems Studied Using Nonlinear Optics
Begin Performance Period: 15-Apr-2017 **End Performance Period:** 14-Apr-2023
Report Term: 0-Other

Submitted By: David Hsieh Email: dhsieh@caltech.edu
Phone: (626) 395-4758

STEM Degrees: 0 **STEM Participants:** 8

Major Goals: Electronic multipolar order is predicted to occur in a variety exotic condensed matter systems including high-Tc superconductors, spin liquids, electronic liquid crystals and heavy fermion superconductors. However, multipolar orders are very challenging to experimentally identify because they are described by tensor order parameters whereas most probes of condensed matter are primarily sensitive to scalar or vector electronic order parameters. The major goal of this project is to explore the coupling of tensor order parameters to high-rank susceptibility tensors, which govern the nonlinear responses of materials, and to use such nonlinear responses to experimentally identify multipolar orders.

This project will focus specifically on nonlinear infrared and optical processes in a variety of materials predicted to host multipolar orders including cuprate based high-Tc superconductors and spin liquids, 4d and 5d transition metal oxides such as the ruthenates, iridates and osmates, and the 4f and 5f electron based heavy fermion systems. Strategies to measure second or third harmonic generation and sum- and difference-frequency generation from these samples will be developed to probe changes in various nonlinear susceptibility tensors across the multipolar ordering transition temperatures and to detect the onset of short-range correlations. We will also theoretically study the coupling between nonlinear optical susceptibility tensors and multipolar order parameters using Landau theory calculations to help interpret the experimental data.

Accomplishments: See uploaded PDF.

Training Opportunities: The postdoc and graduate students working on this project have been provided the following opportunities for training and professional development: 1) Regular meetings with the PI to discuss career paths and weekly meetings with the entire research group to discuss progress and future directions. 2) Collaborations with other postdocs, graduate and undergraduate students in the PI's group to help develop teaching and mentoring skills. 3) Collaboration with external theory or materials synthesis groups to develop project management skills. 4) Participation and presentation of results at conferences, workshops and invited university talks.

RPPR Final Report
as of 31-Jul-2023

Results Dissemination: Results from this project were disseminated via talks and presentations at professional conferences and workshops, which includes the APS March Meeting, the Gordon Research Conference on Novel Trends in Superconductivity of Correlated Electrons, the Conference on Strongly Correlated Electron Systems (SCES), the Conference on Ultrafast Spectroscopy of Correlated Quantum Materials (USCQM), and the Simons Foundation workshop on “Harnessing Light-Matter Interactions in Quantum Materials”. Results were also presented at various university colloquia and seminars, publication in scientific journals and outreach initiatives. See “Products” section for the publications list.

Honors and Awards: 2021 Brown Investigator Award
2022 Moore Experimental Physics Investigator

Protocol Activity Status:

Technology Transfer: Nothing to Report

PARTICIPANTS:

Participant Type: PD/PI
Participant: David Hsieh
Person Months Worked: 1.00 **Funding Support:**
Project Contribution:
National Academy Member: N

Participant Type: Postdoctoral (scholar, fellow or other postdoctoral position)
Participant: Kyle Seyler
Person Months Worked: 3.00 **Funding Support:**
Project Contribution:
National Academy Member: N

Participant Type: Graduate Student (research assistant)
Participant: Daniel Van Beveren
Person Months Worked: 1.00 **Funding Support:**
Project Contribution:
National Academy Member: N

ARTICLES:

RPPR Final Report
as of 31-Jul-2023

Publication Type: Journal Article Peer Reviewed: Y **Publication Status:** 1-Published
Journal: Nature Physics
Publication Identifier Type: DOI Publication Identifier: 10.1038/s41567-021-01210-6
Volume: Issue: First Page #:
Date Submitted: 4/7/21 12:00AM Date Published:
Publication Location:
Article Title: Mirror symmetry breaking in a model insulating cuprate
Authors: A. de la Torre, K. L. Seyler, L. Zhao, S. Di Matteo, M. S. Scheurer, Y. Li, B. Yu, M. Greven, S. Sachdev,
Keywords: Mott insulators, cuprates, multipolar order
Abstract: nderstanding the complex phase diagram of cuprate superconductors is an outstanding challenge. The most actively studied questions surround the nature of the pseudogap and strange metal states and their relationship to superconductivity. In contrast, there is general agreement that the low energy physics of the Mott insulating parent state is well captured by a two-dimensional spin S = 1/2 antiferromagnetic (AFM) Heisenberg model. However, recent observations of a large thermal Hall conductivity in several parent cuprates appear to defy this simple model and suggest proximity to a magneto-chiral state that breaks all mirror planes perpendicular to the CuO2 layers. Here we use optical second harmonic generation to directly resolve the point group symmetries of the model parent cuprate Sr2CuO2Cl2. We report evidence of an order parameter ? that breaks all perpendicular mirror planes and is consistent with a magneto-chiral state in zero magnetic field. Although ? is clearly coupled to the
Distribution Statement: 1-Approved for public release; distribution is unlimited.
Acknowledged Federal Support: **Y**

Publication Type: Journal Article Peer Reviewed: Y **Publication Status:** 1-Published
Journal: Phys. Rev. Research
Publication Identifier Type: DOI Publication Identifier: 10.1103/PhysRevResearch.2.013055
Volume: 2 Issue: First Page #: 013055
Date Submitted: 8/23/20 12:00AM Date Published: 1/16/20 8:00AM
Publication Location:
Article Title: Valence bond phases of herbertsmithite and related copper kagome materials
Authors: M. R. Norman, N. J. Laurita, D. Hsieh
Keywords: spin liquids
Abstract: Recent evidence from magnetic torque, electron spin resonance, and second harmonic generation indicate that the prototypical quantum spin liquid candidate, herbertsmithite, has a symmetry lower than its x-ray refined trigonal space group. Here we consider known and possible distortions of this mineral class, along with related copper kagome oxides and fluorides, relate these to possible valence bond patterns, and comment on their relevance to the physics of these interesting materials.
Distribution Statement: 1-Approved for public release; distribution is unlimited.
Acknowledged Federal Support: **Y**

RPPR Final Report
as of 31-Jul-2023

Publication Type: Journal Article Peer Reviewed: N **Publication Status:** 4-Under Review
Journal: under review
Publication Identifier Type: Publication Identifier:
Volume: Issue: First Page #:
Date Submitted: 8/23/20 12:00AM Date Published:
Publication Location:
Article Title: Evidence for a Parity Broken Monoclinic Ground State in the S = 1/2 Kagomé Antiferromagnet Herbertsmithite
Authors: N. J. Laurita, A. Ron, J. W. Han, A. Scheie, J. P. Sheckelton, R. W. Smaha, W. He, J.-J. Wen, J. S. Lee,
Keywords: spin liquid
Abstract: Nearest-neighbor interacting S = 1/2 spins on the ideal Kagomé lattice are predicted to form a variety of novel quantum entangled states, including quantum spin-liquid (SL) and valence bond solid (VBS) phases. In real materials, the presence of additional perturbative spin interactions may further expand the variety of entangled states, which recent theoretical analyses show are identifiable through the spontaneous loss of particular discrete point group symmetries. Here we comprehensively resolve the ground state point group symmetries of the prototypical Kagomé SL candidate ZnCu3(OH)6Cl2 (Herbertsmithite) using a combination of optical ellipsometry and wavelength-dependent multi-harmonic optical polarimetry. We uncover a subtle parity breaking monoclinic structural distortion at a temperature above the nearest-neighbor exchange energy scale. Surprisingly, the parity-breaking order parameter is dramatically enhanced upon cooling and closely tracks the build-up of nearest-neighbor spin
Distribution Statement: 1-Approved for public release; distribution is unlimited.
Acknowledged Federal Support: **Y**

Publication Type: Journal Article Peer Reviewed: Y **Publication Status:** 1-Published
Journal: Physical Review B (Rapid Communication)
Publication Identifier Type: DOI Publication Identifier: 10.1103/PhysRevB.102.201113
Volume: 102 Issue: First Page #: 201113(R)
Date Submitted: 8/27/21 12:00AM Date Published: 11/13/20 8:00AM
Publication Location:
Article Title: Spin-orbit-enhanced magnetic surface second-harmonic generation in Sr2IrO4
Authors: K. L. Seyler, A. de la Torre, Z. Porter, E. Zoghlin, R. Polski, M. Nguyen, S. Nadj-Perge, S. D. Wilson, D.
Keywords: second harmonic generation, mott insulators
Abstract: An anomalous optical second-harmonic generation (SHG) signal was previously reported in Sr2IrO4 and attributed to a hidden odd-parity bulk magnetic state. Here we investigate the origin of this SHG signal using a combination of bulk magnetic susceptibility, magnetic-field-dependent SHG rotational anisotropy, and overlapping wide-field SHG imaging and atomic force microscopy measurements. We find that the anomalous SHG signal exhibits a two-fold rotational symmetry as a function of in-plane magnetic field orientation that is associated with a crystallographic distortion. We also show a change in SHG signal across step edges that tracks the bulk antiferromagnetic stacking pattern. These results altogether show that the anomalous SHG signal in parent Sr2IrO4 originates from a surface-magnetization-induced electric-dipole process that is enhanced by strong spin-orbit coupling, rather than from a bulk hidden order.
Distribution Statement: 3-Distribution authorized to U.S. Government Agencies and their contractors
Acknowledged Federal Support: **Y**

RPPR Final Report
as of 31-Jul-2023

Publication Type: Journal Article Peer Reviewed: Y **Publication Status:** 1-Published
Journal: Physical Review B
Publication Identifier Type: DOI Publication Identifier: 10.1103/PhysRevB.104.035138
Volume: 104 Issue: 3 First Page #:
Date Submitted: 8/27/21 12:00AM Date Published: 7/1/21 7:00AM
Publication Location:
Article Title: Implications of second harmonic generation for hidden order in
Authors: A. de la Torre, S. Di Matteo, D. Hsieh, M. R. Norman
Keywords: Cuprates, Mott insulators, second harmonic generation
Abstract: Sr2CuO2Cl2 (SCOC) is a model undoped cuprate with I4/mmm crystallographic symmetry, and a simple magnetic space group CAmca with associated magnetic point group mmm1?. However, recent second harmonic spectroscopy in the antiferromagnetic phase has challenged this picture, suggesting instead a magnetic point group 4/mm?m? that coexists with the antiferromagnetism and breaks the two orthogonal mirror planes containing the tetragonal c axis. Here, we analyze the symmetry of SCOC in light of the second harmonic results, and discuss possible ground states that are consistent with the data.
Distribution Statement: 1-Approved for public release; distribution is unlimited.
Acknowledged Federal Support: **Y**

Publication Type: Journal Article Peer Reviewed: Y **Publication Status:** 1-Published
Journal: Annual Review of Condensed Matter Physics
Publication Identifier Type: DOI Publication Identifier: 10.1146/annurev-conmatphys-031218-01371
Volume: 12 Issue: 1 First Page #: 247
Date Submitted: 8/27/21 12:00AM Date Published: 3/1/21 8:00AM
Publication Location:
Article Title: Topology and Symmetry of Quantum Materials via Nonlinear Optical Responses
Authors: J. Orenstein, J.E. Moore, T. Morimoto, D.H. Torchinsky, J.W. Harter, D. Hsieh
Keywords: photogalvanic effects, nonlinear optical effects, second-harmonic generation
Abstract: We review recent progress in the study of photogalvanic effects and optical second-harmonic generation in topological and noncentrosymmetric metals.
Distribution Statement: 1-Approved for public release; distribution is unlimited.
Acknowledged Federal Support: **Y**

Publication Type: Journal Article Peer Reviewed: Y **Publication Status:** 1-Published
Journal: Physical Review B
Publication Identifier Type: DOI Publication Identifier: 10.1103/PhysRevB.106.L140403
Volume: 106 Issue: First Page #: L140403
Date Submitted: 7/16/23 12:00AM Date Published: 10/12/22 7:00AM
Publication Location:
Article Title: Direct visualization and control of antiferromagnetic domains and spin reorientation in a parent cuprate
Authors: K. L. Seyler, A. Ron, D. Van Beveren, C. R. Rotundu, Y. S. Lee, D. Hsieh
Keywords: antiferromagnetism, optical second harmonic generation, domain dynamics
Abstract: We report magnetic optical second-harmonic generation (SHG) polarimetry and imaging on Sr2Cu3O4Cl2, which allows direct visualization of the mesoscopic antiferromagnetic (AFM) structure of a parent cuprate. Temperature- and magnetic-field-dependent SHG reveals large domains with 90? relative orientations that are stabilized by a combination of uniaxial magnetic anisotropy and the Earth's magnetic field. Below a temperature TR ? 97 K, we observe an unusual 90? spin reorientation transition, possibly driven by competing magnetic anisotropies of the two copper sublattices, which swaps the AFM domain states while preserving the domain structure. This allows deterministic switching of the AFM states by thermal or laser heating. Near TR, the domain walls become exceptionally responsive to an applied magnetic field, with the Earth's field sufficient to completely expel them from the crystal. Our findings unlock opportunities to study and apply the mesoscopic AFM behavior of parent cuprates.
Distribution Statement: 2-Distribution Limited to U.S. Government agencies only; report contains proprietary info
Acknowledged Federal Support: **Y**

RPPR Final Report
as of 31-Jul-2023

Publication Type: Journal Article Peer Reviewed: N **Publication Status:** 4-Under Review
Journal: Nature Communications
Publication Identifier Type: Publication Identifier:
Volume: Issue: First Page #:
Date Submitted: 7/16/23 12:00AM Date Published:
Publication Location:
Article Title: A coherent phonon-induced hidden quadrupolar ordered state in Ca2RuO4
Authors: Honglie Ning, Omar Mehio, Xinwei Li, Michael Buchhold, Mathias Driesse, Hengdi Zhao, Gang Cao, Da
Keywords: spin nematic order, quadrupolar order, optical switching
Abstract: Impulsive laser excitation provides a means to transiently realize long-range ordered electronic states of matter that are hidden in thermal equilibrium. Recently, this approach has unveiled a vari- ety of thermally inaccessible ordered states in strongly correlated materials, including charge density wave, ferroelectric, magnetic, and intertwined charge-orbital ordered states. However, more exotic hidden states exhibiting higher multipolar ordering remain elusive owing to the challenge of directly manipulating and detecting them with light. Here we demonstrate a method to induce a dynami- cal transition from a thermally allowed to a thermally forbidden spin-orbit entangled quadrupolar ordered state in Ca2RuO4 by coherently exciting a phonon that is strongly coupled to the order parameter.
Distribution Statement: 2-Distribution Limited to U.S. Government agencies only; report contains proprietary info
Acknowledged Federal Support: **Y**

Partners

,

I certify that the information in the report is complete and accurate:
Signature: David Hsieh
Signature Date: 7/16/23 9:19AM

Summary of Accomplishments (Apr. 15 2017 – Apr. 14 2023)

1. Spin-orbit-enhanced surface magnetic SHG in Sr_2IrO_4

The strongly spin-orbit coupled Mott insulator Sr_2IrO_4 exhibits an anomalous optical second harmonic generation (SHG) signal in zero magnetic (H) field[1], which was previously interpreted as a signature of a hidden bulk magneto-electric order parameter[2]. With support from this award, we developed a rotating (H)-field rotational anisotropy (RA) SHG apparatus. Using a multi-technique approach that includes H-dependent RA-SHG, magnetic susceptibility, wide-field SHG imaging, and atomic force microscopy, we showed that the anomalous SHG signal in Sr_2IrO_4 does not arise from hidden[1] or laser-induced metastable[2] states as previously proposed, but rather from a spin-orbit-enhanced surface response of its bulk antiferromagnetic state [Fig. 1(a)].

By measuring temperature dependent SHG intensities at zero, low, and high H-fields [Fig. 1(b)-(d)], we show that there are three contributions to the finite field SHG response: a crystallographic electric quadrupole (EQ) term, the anomalous term, and a bulk magnetization-dependent term that is strongly enhanced in the high-field spin-flopped $+ + + +$ state [Fig. 1(a)]. These data rule out the possibility of the sample already being in a laser-induced metastable $+ + + +$ state at zero field. We also rule out other proposed laser-induced states by reproducing our data using very weak laser power, as well as showing a transient suppression (rather than enhancement) of SHG intensity following an ultrafast laser excitation. By systematically measuring RA-SHG patterns as a function of the in-plane field angle, we show that the anomalous contribution rotates by 180° upon reversing the field direction ($H \rightarrow -H$) [Fig. 1(e)]. This indicates that the anomalous term does not originate from a magneto-electric order parameter, which generally does not couple linearly to H. Our field-angle-dependent SHG measurements and thermal cycle SHG tests [Fig. 1(j)] also reveal signatures of an underlying 2-fold rotational symmetry that persists in the high-temperature paramagnetic phase, which may be related to a crystallographic symmetry reduction[3,4] or a potential nematic phase that onsets above the Néel temperature[5].

Using a unique approach of overlapping atomic force microscopy and SHG imaging, we find that the SHG patch boundaries do not shift under repeated thermal cycles and many boundaries correlate with structural terraces of the otherwise atomically flat cleaved surface [Fig. 1(f)]. However, a few of the patch boundaries are not associated with topographic steps. To determine the correlation between the order parameter orientation and the topography, we carefully studied a region where four distinct SHG patches intersect [Fig. 1(h)]. Across the SHG boundary without any corresponding step edges [Fig. 1(i)], the order parameter rotates by 90°, consistent with the presence of crystallographic twinning[3]. On the other hand, across a bilayer terrace step,

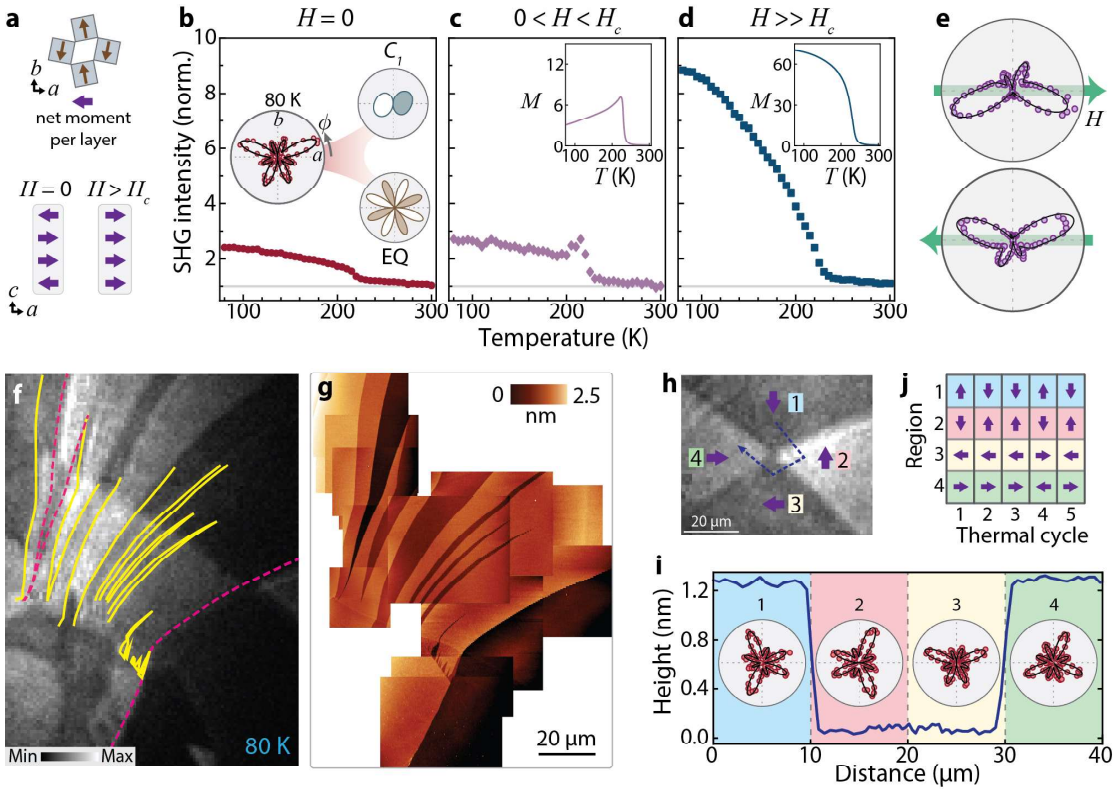

Figure 1. (a) Intralayer Néel order of the J_{eff} = 1/2 pseudospins and the c-axis stacking pattern of the net in-plane moments (purple arrows) at H = 0 (− + + −) and H > H_c (+ + + +). Temperature dependence of SHG intensities for (b) H = 0 mT, (c) 75 mT, and (d) 370 mT. Insets: (b) RA data measured at 80 K and 0 T, which is produced by the interference between a crystallographic EQ term with an anomalous electric dipole term as illustrated on the right. Filled (white) lobes denote opposite optical phase. (d) Magnetization curves for 30 mT and (d) 370 mT in units of 10^{-3} μ_B/Ir. (e) RA-SHG patterns at 80 K and 370 mT for two different applied magnetic field angles 180° apart. (f) SHG image of (001) cleaved Sr_2IrO_4 at 0 T. (g) Composite image of several atomic force microscopy height maps. The yellow solid (magenta dashed) lines in (f) mark where a monolayer (bilayer) step was observed in the height maps. (h) Zoomed-in SHG image at 80 K and 0 T. The local orientations of the anomalous order parameter (purple arrows) were determined by scanning RA measurements. (i) Atomic force microscopy height profile along a line cut shown by the dashed line in (h). Insets show the local RA pattern in each region. (j) Order parameter orientation at 80 K in each of the four regions after successive thermal cycles from 80 K → 295 K → 80 K.

we find an order parameter rotation of 180° [Fig. 1(i)] with anti-correlated flips upon thermal cycling [Fig. 1(j)]. These results confirm a surface-magnetization-induced electric-dipole SHG process from the established − + + − stacking. Such strong magnetic surface SHG, especially from a quasi-2D material that only weakly breaks inversion symmetry at its surface, is very surprising. Since the magnetic surface nonlinear susceptibility scales with spin-orbit coupling, this enhanced surface SHG response is proposed to be enhanced in 5*d* transition metal oxides. These results are published in K. L. Seyler *et al.*, *Phys. Rev. B* **102**, 201113(R) (2020).

2. Hidden multipolar order in $Sr_2CuO_2Cl_2$

Previous work reported evidence of bulk magnetic quadrupolar order in the pseudogap region of the hole-doped cuprate $YBa_2Cu_3O_y$ using RA-SHG[6]. However, it is unclear whether this order only emerges upon destabilizing the parent antiferromagnetic Néel phase by hole doping, or whether it already co-exists with the Néel phase at zero doping. To address this question, we studied $Sr_2CuO_2Cl_2$, a highly tetragonal cuprate parent compound with a Néel temperature of T_N ~ 230 K[7]. Although these crystals cannot be cleaved, we successfully polished flat (001) surfaces that are amenable to RA-SHG measurements.

At room temperature ($T > T_N$), the SHG signal derives from a bulk electric-quadrupole process respecting tetragonal 4/*mmm* symmetry [Fig. 2(a)]. This was established through a series of wavelength-dependent SHG experiments on $Sr_2CuO_2Cl_2$ single crystals. In particular, SHG measurements performed using 800 nm (~1.55 eV) and 1200 nm (~1 eV) incident light [Fig. 2(a)] showed a dramatic difference in SHG efficiency, consistent with the former process being resonant with an electric-dipole forbidden Cu *d-d* transition and the latter being mediated by virtual processes as the probe light lies within the charge gap of $Sr_2CuO_2Cl_2$[8]. Further confirmation was provided by SHG measurements under normal incidence geometry, which showed no SHG signal, consistent with expectations for electric quadrupole SHG radiation. For $T < T_N$, we surprisingly found that the RA-SHG data is not consistent with the symmetries of either the crystallographic or magnetic point groups of $Sr_2CuO_2Cl_2$. To uncover the source of this new SHG process, we performed angle-of-incidence dependent SHG measurements and again found no signal at normal incidence, thus ruling out an electric-dipole radiation source. Interestingly, we also performed spatial dependent SHG polarimetry measurements and found no evidence of magnetic domains. By performing a detailed theoretical analysis, we identified two possible scenarios: a net ferromagnetic dipolar order or an electronic octupolar order that results in a symmetry reduction to a 4/*mm′m′* magnetic point group, breaking the mirror symmetries but preserving the 4-fold rotational symmetry of the crystal [Fig. 2(b)]. The latter is consistent with the point group symmetry of a loop current (magnetic multipolar) order for tetragonal cuprates. Our results were reported in the pair of papers A. de la Torre *et al*., *Nature Phys.* **17**, 777 (2021) and A. de la Torre *et al*., *Phys. Rev. B* **104**, 035138 (2021).

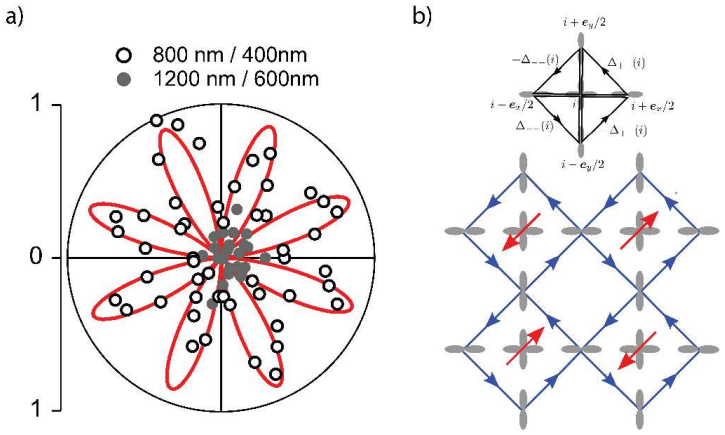

Figure 2. (a) Radially integrated RA-SHG data acquired with 800 nm (white markers) and 1200 nm (grey markers) incident light at $T > T_N$. The red line is a fit to a bulk electric quadrupole SHG term refined under the 4/mmm tetragonal point group. (b) Schematic of a loop current order with symmetry 4/mm′m′.

3. A nematic spin-liquid ground state in $ZnCu_3(OH)_6Cl_2$

Herbertsmithite - $ZnCu_3(OH)_6Cl_2$ - has been reported to host pristine Kagome planes[9] (point group $\bar{3}m$) of highly frustrated spin-1/2 Cu^{2+} ions and is therefore a leading candidate to host a quantum spin-liquid ground state[10]. However, our RA-SHG measurements revealed that its symmetry is lower than the reported centrosymmetric $\bar{3}m$ point group. Instead, a global refinement of the RA-SHG data [Fig. 3(a)] showed that the SHG response was best reproduced by a crystallographic electric dipole SHG process in one of the non-centrosymmetric subgroups of $\bar{3}m$, namely m, $3m$, and 2. To rule out a surface origin for the observed SHG intensity, we performed third harmonic generation (THG) experiments at normal incidence, which are not particularly

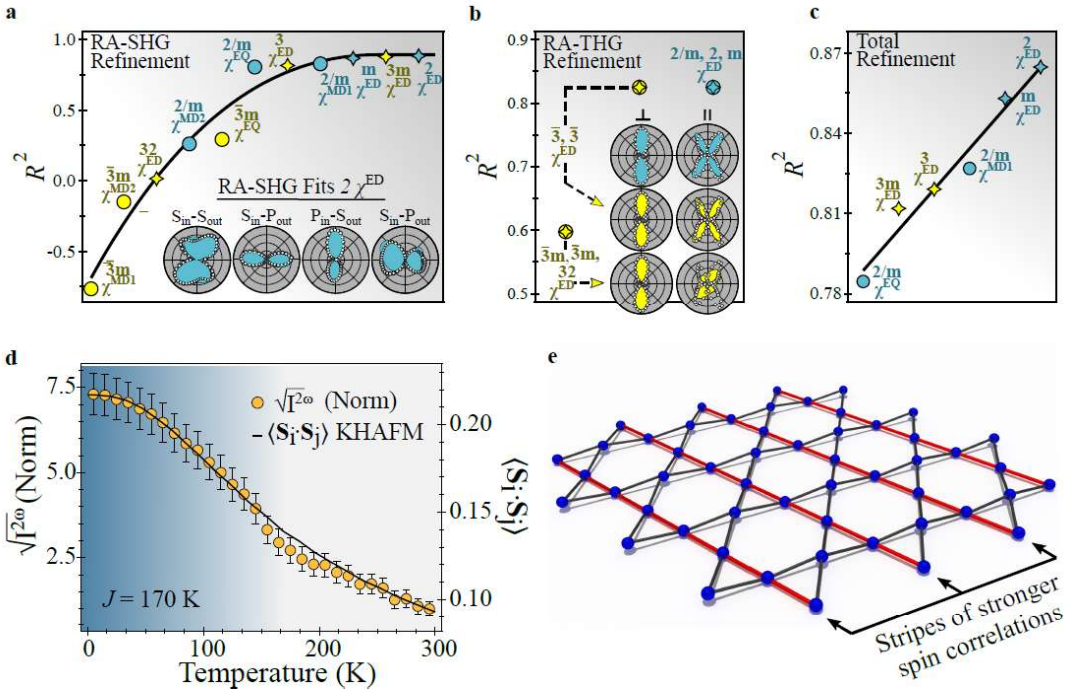

Figure 3. (a) Global refinement of the radially integrated RA-SHG data for non-linear optical processes (ED: electric-dipole, MD: magnetic-dipole, EQ: electric quadrupole) permitted in the refined $\bar{3}$m point group and its subgroups, as captured by the coefficient of determination R^2. Inset displays a fit to an ED response in the point group 2. (b) Similar refinement of the RA-THG data measured at normal incidence. The parallel or perpendicular symbols denote the relative orientation of the incoming and outgoing beam polarization. (c) Total refinement of the entirety of our RA data formed by a weighted average of the R^2values from the RA-SHG and RA-THG refinements as $R^2_{Tot} = (2R^2_{SHG} + R^2_{THG})/3$, favoring monoclinic 2 or m symmetry in Herbertsmithite. (d) Comparison of the observed SHG intensity to the theoretically calculated [11] short-range spin correlator for S = ½ spins on the Kagome lattice. (e) Depiction of the striped spin-liquid phase[12] on a monoclinically deformed Kagome lattice which results in stripes of stronger spin correlations along one of the three formerly equivalent directions of the Kagome plane.

sensitive to surfaces or inversion symmetry and therefore provide insight into the global symmetries of the crystal. Much like the RA-SHG data, the RA-THG data were also found to be inconsistent with the reported $\bar{3}m$ symmetry of Herbertsmithite [Fig. 3(b)], thereby indicating a global distortion. This observation was further corroborated by additional wavelength dependent SHG measurements performed in transmission geometry. To ascertain which point group best reproduces the entirety of our RA data, we formed a weighted average of the refinements of our RA-SHG and RA-THG data [Fig. 3(c)], which favored monoclinic 2 or m symmetry in Herbertsmithite. This indicates not only the absence of inversion symmetry but also a breaking of the three-fold rotational symmetry of the Kagome planes. Given that no change in symmetry of the RA patterns was observed upon cooling, we can also conclude that this distortion already exists above room temperature.

The temperature dependence of the SHG intensity closely follows the theoretically predicted short-range spin correlator on the Kagome lattice[11] [Fig. 3(d)], implying that the build-up of short-range spin correlations dramatically enhances the inversion breaking monoclinic distortion of Herbertsmithite. Our theoretical calculations show that while several distinct deformations of the Kagome lattice could result in monoclinic symmetry, only one such distortion matches a known spin-liquid instability on the Kagome lattice, namely a striped Z_2 nematic spin-liquid phase[12] [Fig. 3(e)]. In this phase, the Kagome lattice buckles so that stripes of shorter Cu^{2+}-Cu^{2+} bonds, and therefore stronger spin correlations, form along one of the three formerly equivalent directions of the Kagome lattice. Our results were reported in the pair of papers N. J. Laurita *et al*., arXiv:1910.13606 and M. R. Norman *et al*., *Phys. Rev. Research* **2**, 013055 (2020).

4. Thermally controlled AFM domain switching in a parent cuprate

The parent compounds of the high-T_c cuprate superconductors are appealing for the exploration of antiferromagnetic (AFM) phenomena due to their model Heisenberg behavior, record-high exchange interactions, and tunability with doping[13,14]. However, there are few works that explore mesoscopic AFM phenomena in the parent cuprates because it is challenging to achieve local readout of AFM order and spatial mapping of AFM domain structures. We showed that optical second-harmonic generation (SHG) can probe AFM domains in the copper oxychloride $Sr_2Cu_3O_4Cl_2$. We also established the existence of magnetization training by the Earth's magnetic field, a domain-dependent uniaxial magnetic anisotropy, and temperature-dependent domain evolution.

We particularly focused on the peculiar domain dynamics around $T_R \sim 97$ K, showing that there exists a previously unresolved magnetic isotropic point. We performed SHG imaging in the vicinity of T_R, which shows the evolution from a two-domain state to a global single-domain state followed by the reappearance of two domains with 90° reoriented magnetizations [Fig. 4(a)]. The spatial dynamics of this phase transition are highly repeatable, thus allowing for deterministic switching between 90° AFM states by simply heating and cooling though T_R [Fig. 4(b)]. Moreover, we found that the transition can be traversed by simply tuning the optical power while keeping the cryostat temperature fixed [Fig. 4(c)]. To better understand the nature of the reorientation transition, we performed anisotropic magneto-SHG (AM-SHG) measurements, which can reveal underlying magnetic anisotropies. At T_R, the AM-SHG pattern shows C_4 symmetry, while above and below T_R there is C_2 symmetry but with a 90° rotation relative to one another [Fig. 4(d)]. This strongly suggests that the reorientation transition at T_R is driven by a sign change in the uniaxial magnetic anisotropy. We developed a theoretical model to explain this, which supposes that spins on the two copper sublattices (Cu_I and Cu_{II}) exhibit temperature-dependent competing in-plane uniaxial magnetic anisotropies that cross at T_R, thus flipping the net anisotropy [Fig. 4(e)]. We also note that spin correlations within the Cu_{II} sublattice have been shown to onset near 100K[15], which could induce magnetoelastic deformations that are relevant to the anisotropy change.

Using SHG imaging under small applied magnetic fields, we directly identified a striking divergence in the domain wall susceptibility at T_R [Fig. 4(f)]. As the net uniaxial anisotropy crosses zero, the 90° domain walls become energetically unfavorable and are easily expelled by small magnetic fields. By the tuning the direction of a small applied magnetic field, we have shown that it possible to prepare a sample-sized single-domain state of a desired orientation [Fig. 4(g)]. Our experiments help to explain the intriguing AFM domain dynamics observed using low-field magnetometry in Ref. 16. More generally, they provide an approach to locally readout AFM states, globally image AFM domain walls, and deterministically switch 90° domains in a cuprate for the first time. These are results are published in K. L. Seyler *et al*., *Phys. Rev. B* **106**, L140403 (2022).

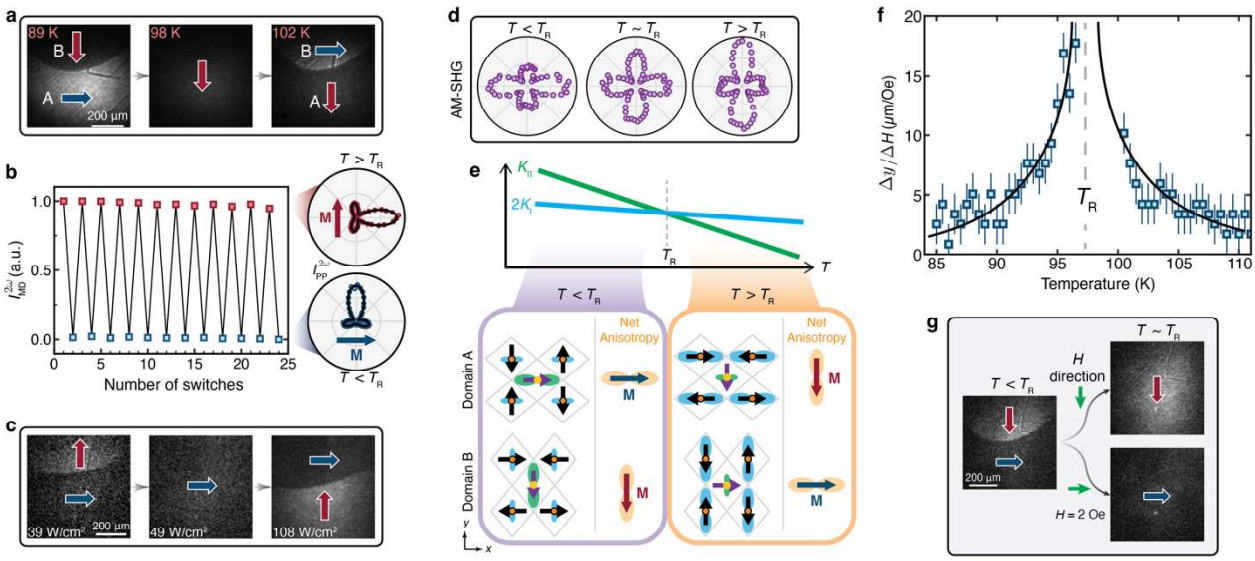

*Figure 4. (a) SHG images acquired upon warming through T_R. Large arrows indicate the magnetization **M**. (b) SHG intensity on domain A under repeated thermal switching through heating to 120 K (red) and cooling to 80 K(blue). Corresponding rotational anisotropy patterns shown on right. (c) SHG images acquired at three different excitation intensities at ~95.5 K. (d) Anisotropic magneto-SHG below, at, and above T_R. (e) Schematic of competing magnetic anisotropies model. The graph depicts how Cu_I and Cu_{II} in-plane spin anisotropies, labelled as K_I and K_{II} respectively, may vary around T_R. In the crystal schematics, the size and orientation of the blue (green) lobes depict the direction and strength of the Cu_I (Cu_{II}) spin anisotropy above and below T_R for domain A and B, which are distorted in different directions. Net anisotropy for **M** is shown on right. (f) Temperature dependence of domain wall motion per change in H-field around T_R. Black lines are guides to the eye. (g) SHG images at T_R for two different directions of a weak H-field (2 Oe).*

5. Ultrafast detection and control of multipolar order in Ca_2RuO_4

The multiband Mott insulator Ca_2RuO_4 has recently been proposed to exhibit excitonic magnetism[17] below $T_N = 110$ K. This occurs because of the comparable energy scales of spin-orbit coupling (SOC) and magnetic exchange, which allows the singlet (effective angular momentum $J = 0$) ground state to spontaneously become magnetic via virtual hopping to the triplet ($J = 1$) state. More intriguingly, a time-reversal-symmetric pseudospin quadrupolar ordered (QO) phase – dubbed a spin-nematic – is predicted to be stabilized below $T_{QO} = 260$ K by the Jahn-Teller (JT) interaction[18]. However, this QO order is "hidden" to conventional probes owing to its lack of a dipolar moment and lack of structural symmetry lowering. We demonstrated that an ultrafast switch of the QO can be identified and impulsively stimulated by sub-gap light excitation at 0.3 eV and probed by broadband energy-resolved coherent phonon spectroscopy.

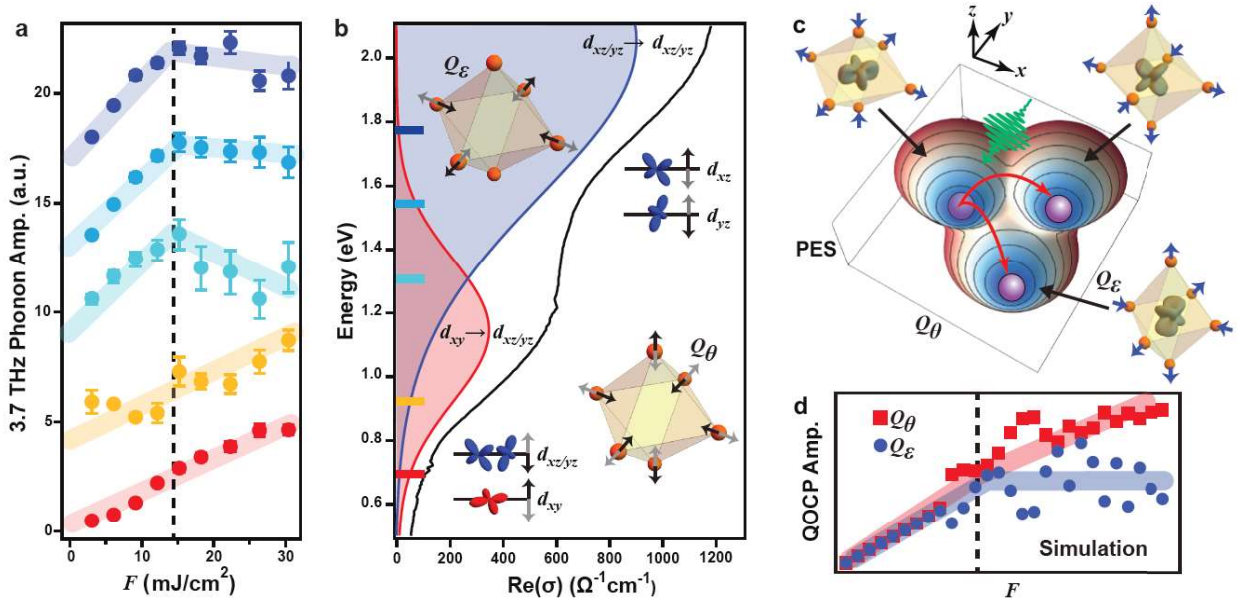

Figure 5.(a) Pump fluence dependence of the 3.7 THz phonon amplitude probed at select energies as denoted by the corresponding color bars in panel b. (b) Optical conductivity digitized from Ref.19. The insets show the real space configuration of the two Q_θ and Q_ε eigenmodes, and their induced modulation of orbital levels. (c) Potential energy surface calculated from the microscopic model. The corresponding real-space pseudospin distribution and lattice distortion for each valley are shown on the side. (d) Calculated pump fluence dependence of the Q_θ and Q_ε amplitudes.

Out of the six Raman-active phonon modes, we found the amplitude of five modes scale linearly with fluence (F) up to at least 30 mJ/cm^2 as expected of conventional impulsively stimulated Raman-active phonons, while a particular 3.7 THz mode shows clear nonlinear scaling above a critical fluence $F_c = 15$ mJ/cm^2 at 80 K. The temperature dependence of both F_c and the 3.7 THz mode amplitude exhibits an order-parameter-like onset at T_{QO}, indicating a direct coupling

of the phonon amplitude nonlinearity to the QO. The nonlinear fluence dependence of 3.7 THz phonon amplitude and its temperature dependence can both be simulated by the many-body microscopic model we developed, as a switch of QO from a ground state with d_{xy}-dominated orbital polarization and tetragonal compression along z-axis to the two excited states with $d_{xz/yz}$-orbital dominated character with compression along the y/x-axis occurs [Fig. 5(c)].

To further study the phonon amplitude nonlinearity with electronic band selectivity, we investigated the F-dependence of the 3.7 THz mode amplitude at various probe photon energies at 80 K. Optical conductivity shows a $d_{xy}\rightarrow d_{xz/yz}$ dominated transition peak between 0.5-1.3 eV and a $d_{xz/yz}\rightarrow d_{xz/yz}$ transition peak between 1.3-2.1 eV within our probe energy range [Fig. 5(b)][19]. The former transition is more susceptible to a tetragonal distortion mode, Q_θ, of the octahedron, since this mode modulates the splitting between d_{xy} and $d_{xz/yz}$. On the other hand, the $d_{xz}\rightarrow d_{yz}$ (or vice versa) transition is more sensitive to the orthorhombic mode, Q_ε, which breaks the in-plane degeneracy and thus swaps the orbital occupation of the d_{xz} and d_{yz} bands without involving d_{xy} [Fig. 5(b) insets]. Therefore, scanning the probe energy from the $d_{xy}\rightarrow d_{xz/yz}$ to $d_{xz/yz}\rightarrow d_{xz/yz}$ transition enables a selective coupling to the Q_θ and Q_ε components of the 3.7 THz phonon, respectively. Intriguingly, for probe energies resonant with the $d_{xy}\rightarrow d_{xz/yz}$ transition edge, the amplitude of the 3.7 THz mode exhibits quasi-linearity up to 30 mJ/cm^2. In contrast, for probe energies resonant with the $d_{xz/yz}\rightarrow d_{xz/yz}$ transition edge, the amplitude displays a clear deviation from linearity at F_c = 15 mJ/cm^2 [Fig. 5(a)]. This clear dichotomy highlights the distinct behavior of the Q_θ and Q_ε modes as the QO is modulated by light, which is corroborated by our theoretical simulations [Fig. 5(d)].

Our work not only expands the field of ultrafast order parameter control to unconventional multipolar orders, but also demonstrates probe-energy dependent coherent phonon spectroscopy as a sensitive probe of hidden orders. A manuscript describing these results is currently in review.

Bibliography

1. Zhao, L. *et al.* Evidence of an odd-parity hidden order in a spin–orbit coupled correlated iridate. *Nat. Phys.* **12**, 32–36 (2016).
2. Di Matteo, S. & Norman, M. R. Magnetic ground state of Sr_2IrO_4 and implications for second-harmonic generation. *Phys. Rev. B* **94**, 075148 (2016).
3. Dhital, C. *et al.* Neutron scattering study of correlated phase behavior in Sr_2IrO_4. *Phys. Rev. B* **87**, 144405 (2013).
4. Ye, F. *et al.* Magnetic and crystal structures of Sr_2IrO_4: A neutron diffraction study. *Phys. Rev. B* **87**, 140406 (2013).

5. Murayama, H. *et al.* Bond directional anapole order in a spin-orbit coupled Mott insulator $Sr_2(Ir_{1-x}Rh_x)O_4$. *Phys. Rev. X* **11**, 011021 (2021).
6. Zhao, L. *et al.* A global inversion-symmetry-broken phase inside the pseudogap region of $YBa_2Cu_3O_y$. *Nat. Phys.* **13,** 250–254 (2017).
7. Vaknin, D., Sinha, S. K., Stassis, C., Miller, L. L. & Johnston, D. C. Antiferromagnetism in $Sr_2CuO_2Cl_2$. *Phys. Rev. B* **41,** 1926–1933 (1990).
8. Choi, H. S. *et al.* Anomalous temperature dependence of charge-transfer excitation in the undoped cuprate $Sr_2CuO_2Cl_2$. *Phys. Rev. B - Condens. Matter Mater. Phys.* **60,** 4646–4652 (1999).
9. Shores, M. P., Nytko, E. A., Bartlett, B. M. & Nocera, D. G. A Structurally Perfect S = 1/2 Kagomé Antiferromagnet. *J. Am. Chem. Soc.* **127**, 13462–13463 (2005).
10. Norman, M. R. Colloquium: Herbertsmithite and the search for the quantum spin liquid. *Rev. Mod. Phys.* **88**, 041002 (2016).
11. Müller, P., Zander, A. & Richter, J. Thermodynamics of the kagome-lattice Heisenberg antiferromagnet with arbitrary spin S. *Phys. Rev. B* **98**, 024414 (2018).
12. Clark, B. K., Kinder, J. M., Neuscamman, E., Chan, G. K.-L. & Lawler, M. J. Striped Spin Liquid Crystal Ground State Instability of Kagome Antiferromagnets. *Phys. Rev. Lett.* **111**, 187205 (2013).
13. Manousakis, E. The spin-1/2 Heisenberg antiferromagnet on a square lattice and its application to the cuprous oxides. *Rev. Mod. Phys.* **63**, 1 (1991).
14. Lee, P. A., Nagaosa, N., Wen, X.-G. Doping a mott insulator: Physics of high-temperature superconductivity. *Rev. Mod. Phys.* **78**, 17 (2006).
15. Kim, Y. J. *et al.* Neutron scattering study of $Sr_2Cu_3O_4Cl_2$, *Phys. Rev. B* **64**, 024435 (2001).
16. Parks, B. *et al.* Magnetization measurements of antiferromagnetic domains in $Sr_2Cu_3O_4Cl_2$. *Phys. Rev. B* **63**, 134433 (2001).
17. Khaliullin, G. Excitonic Magnetism in Van Vleck–type d^4 Mott Insulators. *Phys. Rev. Lett*. **111**, 197201 (2013).
18. Liu, H. & Khaliullin, G. Pseudo-Jahn-Teller Effect and Magnetoelastic Coupling in Spin-Orbit Mott Insulators. *Phys. Rev. Lett.* **122**, 057203 (2019).
19. Jung, J. H. *et al*. Change of electronic structure in Ca_2RuO_4 induced by orbital ordering. *Phys. Rev. Lett.* **91**, 056403 (2003).